Mechanics and Mechanical Engineering
Vol. 15, No. 3 (2011) 333–341

Flutter Analysis of IV Standard Configuration Cascades, Direct Integration Method

Romuald Rządkowski
The Szewalski Institute of Fluid Machinery
Polish Academy of Sciences
z3@imp.gda.pl

Leszek Kubitz
Polish Naval Academy
L.Kubitz@amw.gdynia.pl

Received (18 August 2011)
Revised (20 September 2011)
Accepted (28 September 2011)

A three–dimensional nonlinear time–marching method and numerical analysis for aeroelastic behaviour of oscillating blade row has been presented. The approach is based on the solution of the coupled fluid–structure problem in which the aerodynamic and structural equations are integrated simultaneously in time. Thus providing the correct formulation of a coupled problem, as the interblade phase angle at which a stability (or instability) would occur, is a part of the solution.

Keywords: Aeroelasticity, fluid structure interaction

1. Introduction

Aeroelasticity phenomena are characterised by the interaction of fluid and structural domains, most prediction methods tend to treat the two domains separately, and they usually assume some critical interblade phase angle for which the flutter analysis is carried out for a single passage.

A review of the literature on flutter prediction methods is beyond the scope of this paper and the interested reader should consult [1]. The unsteady prediction models for 3D non-viscous and viscous flutter have been discussed in literature over the last ten years (see for example [2], [3], [4], [5], [6], [7], [8], [9], [10], [11], and [12]).

The traditional approach in flutter calculations of bladed disks is based on frequency domain analysis ([13], [14], and [15]), in which the blade motions are assumed to be harmonic functions of time with a constant phase lag between adjacent blades, and the mode shapes and frequencies are obtained from structural computations. This approach ignores the feedback effect of the fluid on the structural vibration.

In recent times, the new approaches based on the simultaneous integration in time of the equations of motion for the structure and the fluid have been developed ([11], [14]; [12], [17], [10]). These approaches are very attractive due to the general formulation of a coupled problem, as the interblade phase angle at which stability (instability) would occur is a part of solution.

For the first time the direct integration method to flutter analysis was used using Wilson–theta method and one dimensional beam theory for 1st Standard Configuration [17].

In the present study the direct integration method was used to calculate the aeroelastic behaviour for a three–dimensional oscillating IV standard configuration blade row in transonic gas flow. The blade was modelled by 20 nodes izoparametric element.

2. Aerodynamic model

The flow model is described in detail in ([18], [10]), a brief summary will be given here for the sake of completeness. It is considered the 3D transonic flow of an ideal gas through a multipassage blade row. In the general case the flow is assumed to be a periodic function from blade to blade (in pitchwise direction), so the calculated domain includes all blades of the whole assembly (Fig.1).

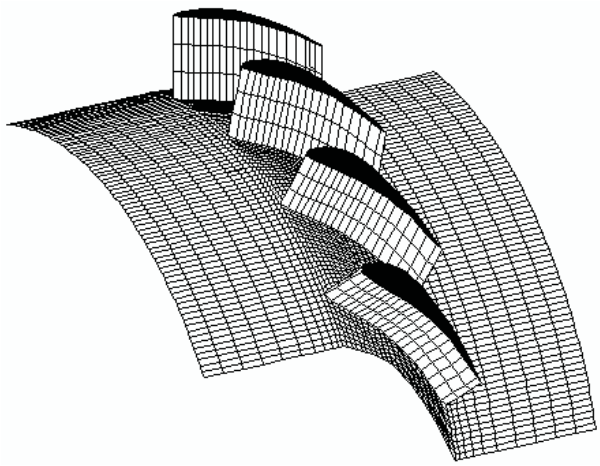

Figure 1 A view of a sector of the whole blade assembly

The flow equations will be written for a three dimensional Cartesian coordinate system which is fixed to a rotating blade row. In this case, the conservative form of the unsteady Euler equations is given ([10]):

$$\frac{\partial}{\partial t}\int\limits_{\Omega} f d\Omega + \oint\limits_{\sigma} \vec{F}\cdot\vec{n}d\sigma + \int\limits_{\Omega} H d\Omega = 0 \tag{1}$$

Here f is the solution vector; $\vec{F}$ is the inviscid flux through the lateral area σ bounding the finite volume Ω, and H is source vector which contains the terms due to the rotation of the coordinate system. The above system of equations is completed by the perfect gas equation

$$p = \rho\,\varepsilon(\chi - 1) \tag{2}$$

where χ denotes the ratio of the fluid specific heats ε is an internal energy of mass unit. The spatial solution domain is discretized using linear hexahedral elements. The equations (1–2) are integrated on moving H–H (or H–O) – type grid with use of explicit monotonous second – order accuracy Godunov – Kolgan difference scheme ([18]).

We assume that the unsteady fluctuations in the flow are due to prescribed blade motions, and the flows far upstream and far downstream from the blade row are at most small perturbations of uniform free streams. So the boundary conditions formulation is based on one – dimensional theory of characteristics, where the number of physical boundary conditions depends on the number of characteristics entering the computational domain.

In the general case, when axial velocity is subsonic, at the inlet boundary initial values for total pressure, total temperature and flow angles are used in terms of the rotating frame of reference, while at the outlet boundary only static pressure has to be imposed. On the blade surface, zero flux is applied across the solid surface (the grid moves with the blade).

Periodic conditions are applied at the upper and lower boundaries of the calculated domain at each time moment. However there are some situations where it is possible to reduce the number of passages used in the calculations. For unsteady flows in which all blades perform harmonic oscillations with the particular mode shape, frequency and a constant interblade phase angle (IBPA) (tuned cascades), the number of blades passages depends on the value of the interblade phase angle. For instance, computations with the phase angle $\delta = \pm\ 90$ deg. can be made for four passages. The time step at the coupled calculations is assumed to be constant and is chosen from the stability conditions of the explicit scheme for the fluid model.

3. Structural model

The structural model is based on 3D finite element blade model and the direct integration method ([16]). Each blade is treated as an individual during the numerical calculations using in–house code. The 20 nodes izoparmateric element was used to model the blade.

Boundary conditions from the structural and aerodynamic domains are exchanged at each time step and the aerodynamic mesh is moved to follow the structure motion (the partially coupled method). The structural damping is not included here. The mesh used to integrate the structural equations is the same as the mash used in the flow code.

4. Numerical results

The numerical calculations have been carried out for the turbine cascade known as the Fourth Standard Configuration, which has been experimentally investigated in the nonrotating annular cascade tunnel in transonic flow ([13]). As the first step the numerical calculations were performed to compare with the experimental ones.

The steady and unsteady predictions have been made on the hybrid H–H type grid with 10 x 30 x 60 grid points including moving H–grid (16 points across) near the blade. In order to compare the results for the unsteady flow, the numerical results for the steady flow must be validated, because they are the starting point for the unsteady flow calculations.

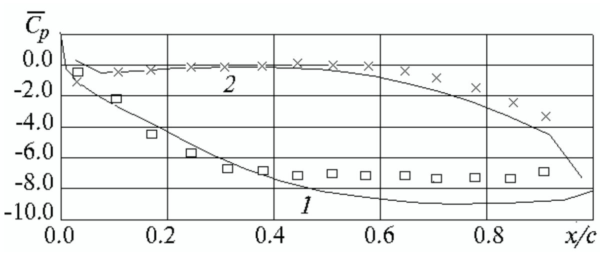

Figure 2 The time averaged pressure coefficient distribution over the blade chord (1 suction side, 2 pressure side, [ ][ ] pressure side experiment, ×× suction side experiment)

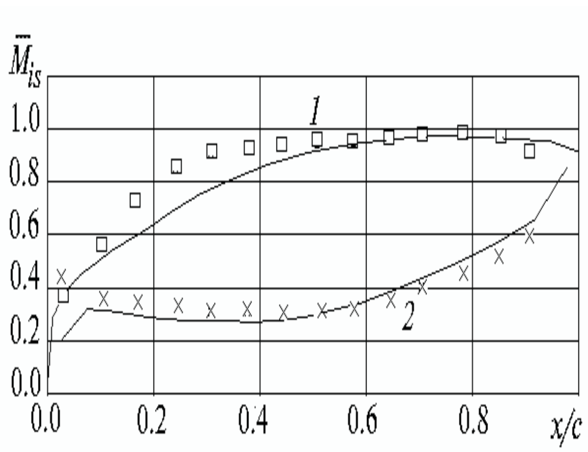

Figure 3 The Mach number (b) distribution over the blade chord (1 suction side, 2 pressure side, [ ][ ] pressure side experiment, ×× suction side experiment)

In Fig. 2 the calculated and experimental results of steady pressure coefficient are presented and in Fig. 3 the distribution of the isentropic Mach number along the middle section of the blade is shown. The integers "1" and "2" corresponds to the suction and pressure sides respectively. Agreement between the numerical and experimental results is quite good. The small discrepancies are noticeable near the leading edge at approximately 30% of the chord length on the suction side.

At 150 Hz excitation, the motion of the 3D blades was the same as in experiment, where the interblade phase angle varied. There the blades moved as a rigid body, and the root section moved with the same amplitude as the periphery section.

In our model we assumed the blades to be cantilever, so their root sections did not move. In order to obtain the same blade amplitude as in the experiment, force was applied to their tip cross–sections. The calculated natural frequencies of the IV Configuration blade were: 4805 Hz, 6541 Hz and 11320 Hz for $E = 2,1 \cdot 10^{11}$ MPa, $\rho = 7850$ kg/m^3.

In the experiment the excitation frequency was equal to 150 Hz, which is not the first natural frequency of the blade. Thus in the model the blade material parameters were changed to $E = 2,0933 \cdot 10^2$ MPa, $\rho = 7850$ kg/m^3 in order to obtain a first natural frequency equal to 150 Hz. The remaining natural frequencies were: 204 Hz, 354 Hz, 436 Hz, 491 Hz, and 705 Hz.

In the aerodynamic test the blades vibrations during experiments were kept constant in time and also between the different blades. The experimentally determined time–averaged blade surface pressure distributions were used to calculate the aerodynamic work.

In this numerical calculation the rotor blades were assumed to be fixed in the root. The blades oscillated in a sinusoidal motion with a constant interblade phase angle.

In the next step the interblade phase angle were no longer kept constant. The blade displacements and velocities and the flow variables in each period of time were used as the initial conditions for the time–integration procedure. The amplitude of blade oscillations could grow or decay.

In this procedure, the blade motion was initially confined to the specific phase angle selected in the initial condition. The blade was initially forced with a phase angle of 90 deg. and an excitation frequency of 150 Hz. Fig. 4 illustrates the motion of four blades with an $f = 150$ Hz excitation frequency and 90 deg phase angle. This phase angle is not one in which flutter appears ([13], [16]). For some time after the blades were released from the assumed interblade phase angle, their motion motion maintained a stable phase angle and their amplitude decayed (Fig. 4). Aerodynamic damping caused the phase angle to constantly change. Transient behaviour was observed near $t = 1,7$ s., when the phase angle changed to an unstable condition and the amplitude started to increase.

Fig. 5 illustrates motion of four blades for $f = 150$ Hz excitation and a -90 deg interblade phase angle. This phase angle is one where flutter appears ([13], [16]). Once the blades were released from the assumed interblade phase angle, the amplitude increased (Fig. 5).

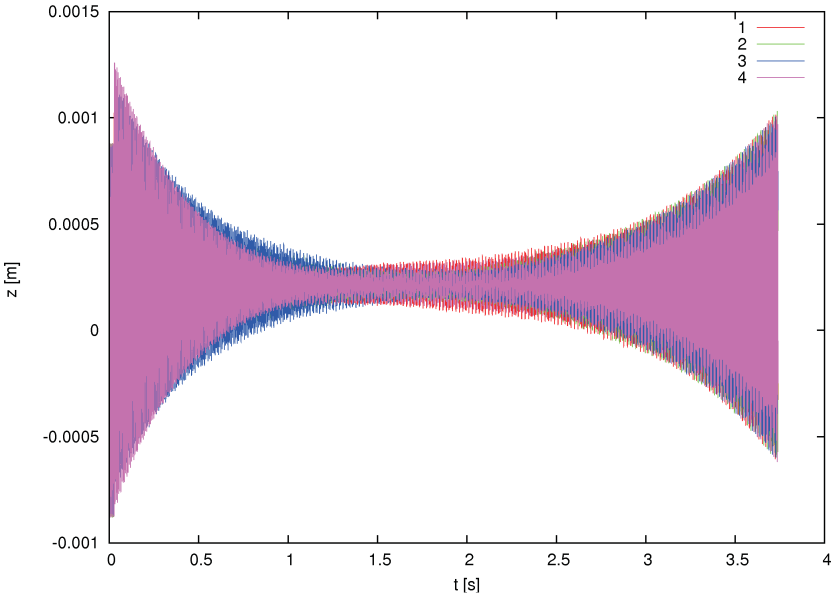

Figure 4 Bending blade motion with 150 Hz excitation frequency and +90 deg phase angle in long time response

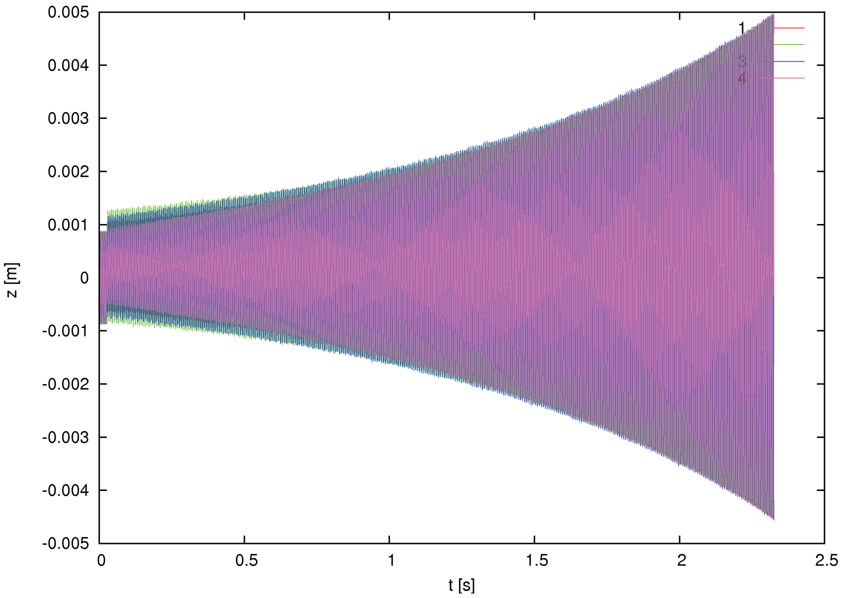

Figure 5 Bending blade motion for 150 Hz excitation frequency and -90 deg phase angle in long time response

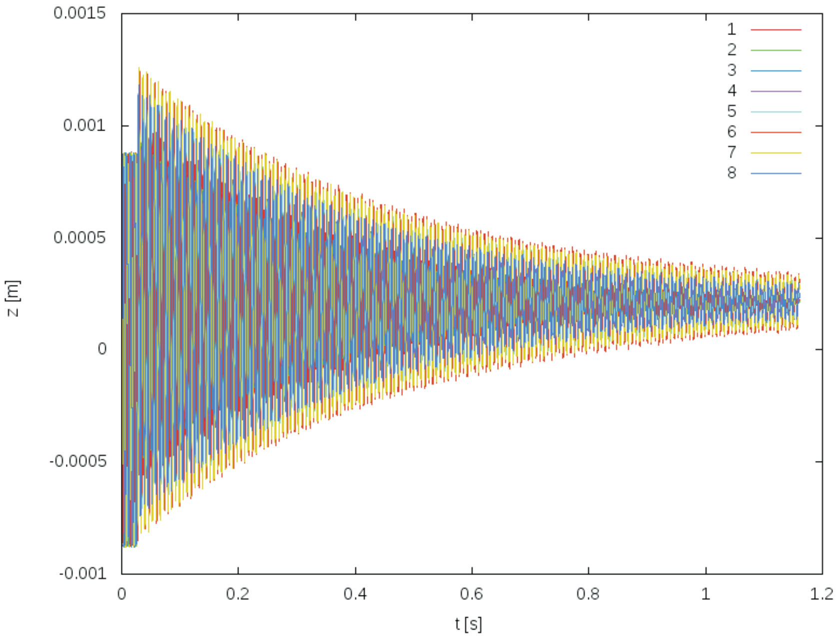

Figure 6 Bending blade motion with 150 Hz excitation frequency and +45 deg phase angle in long time response

Next the motion of 8 blades were analyzed for interblade phase angle equal to 45 deg. Fig. 6 illustrates blades motion for the excitation frequency $f = 150$ Hz and the phase angle 45 deg. This phase angle is not the critical values obtained in the frequency domain analysis ([13], [16]). After blades being released from the assumed interblade phase angle, the blade motion shows the same phase angle and the amplitude decays.

The motion of the blade for interblade phase angle equal to -45 deg was different due the fact that similar as in Fig. 5.

Thus it is clear that the time domain method predicts the same interblade phase angle value as the frequency domain method. It is interesting to observe that by the using time domain method flutter appears even in blades initially moving with a stable inter–blade angle.

5. Conclusions

In this study the simultaneous time domain method was used to determine the aeroelastic stability of a cascade. The unsteady equations of motion for the structure and the fluid were simultaneously integrated, starting with a steady flowfield. Each blade was allowed to move independently, and the motion of all blades was analyzed to determine their aeroelastic stability.

Good agreement between the experimental and numerical results was observed for the assumed sinusoidal blade motion and fixed interblade phase angle.

For the fully coupled fluid–structure problem in which only the interblade phase angle was assumed as the initial condition it was found that for non-critical interblade phase angles equal to 90 deg the blade amplitude first decreased and then increased. The interblade phase angle changed from a stable condition to an unstable one.

The direct integration method gives us a much more precise tool for flutter analysis than the frequency domain method.

Acknowledgement

The authors wish to acknowledge KBN for the financial support of this work (project PB4798/B/T02/2010/38).

All numerical calculations were made at the Academic Computer Centre TASK (Gdansk, Poland).

References

[1] **Marshall, J.G. and Imregun M.**: A Review of Aeroelasticity Methods with Emphasis on Turbomachinery Applications, *Journal of Fluids and Structures*, Vol. 10, 237–257, **1996**.

[2] **Sayma, A.I., Vahdati, M., Green, J.S. and Imregun, M.**: Whole – Assembly Flutter Analysis of a Low Pressure Turbine Blade, *in book T.H. Fransson ed.: Unsteady Aerodynamics and Aeroelasticity of Turbomachines*, Proceedings of the 8^{th} International Symposium held in Stockholm, Sweden, 14–18 September 1997, Kluwer Academic Publishers, 347–359, **1998**.

[3] **Weber, S., Gallus, H.E. and Peitsch, D.**: Numerical Solution of the Navier Stokes Equations for Unsteady Unstalled and Stalled Flow in Turbomachniery Cascade with Oscillating Blades, *in book T.H. Fransson ed.: Unsteady Aerodynamics and Aeroelasticity of Turbomachines*, Proceedings of the 8^{th} International Symposium held in Stockholm, Sweden, 14–18 September 1997, Kluwer Academic Publishers, 478–491, **1998**.

[4] **Vasanthakumar, P., Chen, T. and He L.**: Three–Dimensional Viscous Computation of Blade Flutter and Forced Response Using Nonlinear Harmonic Approach, *in book P. Farrand, S. Auber : Unsteady Aerodynamics, Aeroacustics and Aeroelasticity of Turbomachines*, Proceedings of the 9th International Symposium held in Lyon, France, 4-8 September 2000, Presses Universitaires de Grenoble, 649–665, **2001**.

[5] **Chassaing, J.C and Gerolymos, G.A.**: Compressor Flutter Analysis Using Time–Nonlinear and Time–Linearized 3–D Navier–Stokes Method, *in book P. Farrand, S. Auber: Unsteady Aerodynamics, Aeroacustics and Aeroelasticity of Turbomachines*, Proceedings of the 9th International Symposium held in Lyon, France, 4-8 September 2000, Presses Universitaires de Grenoble, 666–677, **2001**.

[6] **McBean, I., Liu, F., Hourigan, K. and Thompson, M.**: Simulation of Aeroelasticity in an Annular Cascade using a Parallel 3–Dimensional Navier–Stokes Solver, *Proceedings of ASME Turbo Expo 2002*, June 2-6, 2002, Amsterdam, GT–2002–30366, **2002**.

[7] **Fransson, T.H., Jöcker, M., Bölcs, A. and Ott, P.**: Viscous and Inviscid Linear/Nonlinear Calculations Versus Quasi–Three–Dimensional Experimental Data for a New Aeroelastic Turbine Standard Configuration, *ASME Journal of Turbomachinery*, 121, 717–725, **1999**.

[8] **Rządkowski, R. and Gnesin, V.**: A 3D Inviscid Self–Excited Vibration of the Last Stage Turbine Blade Row, *Journal of Fluids and Structures*, 23, 858–873, **2007**.

[9] **Rządkowski, R., Gnesin, V. and Kolodyazhnaya, L.**: 3D Viscous Flutter of 11th Configuration Blade Row, *Advances in Vibration Engineering*, 8(3), 213–228, **2009**.

[10] **Gnesin, V., Rządkowski, R. and Kolodyazhnaya, L.**: A Coupled Fluid–Structure Analysis for 3D Flutter in Turbomachines, *Proceedings of the ASME Turbo Expo 2000*, May 8–11, Munich, Germany, CD–ROM, Structures &Dynamics, SD–06, 2000–GT–380, **2000**.

[11] **Bakhle, M.A., Reddy, T.S.R., and Keith T.G.**: Time Domain Flutter Analysis of Cascades Using a Full–Potential Solver, *AIAA J.* vol.30, No 1, p.163, **1992**.

[12] **Bendiksen, O.O.**: Nonlinear Blade Vibration and Flutter in Transonic Rotors, *Proc. of ISROMAC - 7*, The 7^{th} Intern. Symp. on Transport Phenomena and Dynamics of Rotating Machinery, Feb., 22–26, Honolulu, Hawaii, USA, p. 664, **1998**.

[13] **Bölcs, A., and Fransson, T.H.**: Aeroelasticity in Turbomachines: Comparison of Theoretical and Experimental Cascade Results, *Communication du LTAT. - EPFL Switzerland*, No 13, 174, **1986**.

[14] **He, L.**: Integration of 2D Fluid / Structure Coupled Systems for Calculation of Turbomachinery Aerodynamic, Aeroelastic Instabilities, *J. of Computational Fluid Dynamics*, vol.3, 217, **1984**.

[15] **Moyroud, F., Jacquet - Richardet, G., and Fransson, T., H.**: A Modal Coupling for Fluid and Structure Analysis of Turbomachine Flutter Application to a Fan Stage, *ASME Paper*, 96 - GT - 335, 1–19, **1996**.

[16] **Rządkowski, R.**: Dynamics of Steam Turbine Blading, Part Two Bladed Discs, *Ossolineum, Wrocław–Warszawa, 1998.*

[17] **Rządkowski, R., Gnesin, V. and Kovalov, A.**: The 2D Flutter of Bladed Disc in an Incompressible Flow, *The 8^{th} International Symposium of Unsteady Aerodynamics and Aeroelasticity of Turbomachines*, Stockholm, Sweden, Sept. 14–18, 317–334, **1997**.

[18] **Sokolovsky, G., A., and Gnesin V.,I.**: Unsteady and Viscous Flows in Turbomachines, *Naukova Dumka, Kiev* (in Russian), **1986**.